





Development of a Single-Seater Electric Vehicle for Electrathon America Competition

Vignaud Granados Alejo ^{1,*}, Francisco Javier Santander Bastida ²,
Alejandra de los Ángeles Guzmán Patiño¹, Pedro Jorge de los Santos Lara ¹,
and Pedro Yañez Contreras ¹

¹ Robotics Engineering, Polytechnic University of Guanajuato, Cortazar Guanajuato, México

² Manufacturing Technology Engineering, Polytechnic University of Guanajuato, Cortazar Guanajuato, México

Email: vgranados@upgto.edu.mx (V.G.A.); fsantander@upgto.edu.mx (F.J.S.B.);

23039019@upgto.edu.mx (A.A.G.P.); jdelossantos@upgto.edu.mx (P.J.S.L.); pyañez@upgto.edu.mx (P.Y.C.)

*Corresponding author

Abstract—Electrathon Americas is an organization that promotes the development of electric vehicles for competition. The present work is focused on the design of the America single-seater structure which was based mainly on the protection of the driver, space for various accessories, improve range and aerodynamics. The design was carried out in strict adherence to the Electrathon America 2021 manual. The 3D Computer Aided Design (CAD) modeling was performed using SolidWorks software. Aluminum and steel profiles with diameters of ½ in and ¾ in with a thickness of 2.7 mm were used. The regulations specify that tests must be performed on the structure of the single-seater, mainly torsion and bending tests to ensure its correct operation with a minimum safety factor of 2; therefore, structural analyses were conducted using Ansys software. Additionally, a fluid analysis was performed. Strain gauges were used to measure structural deformations in order to validate the stress analyses carried out on the single-seater chassis. A functional single-seater vehicle was obtained, featuring a structure with a safety factor of 1.7, improvement aerodynamic, suspension and adequate steering, achieving a range of 38 km with a 1 kWh battery according to Electrathon guidelines, as well as a total mileage of 200 km without failures.

Keywords—design, America single-seater, Ansys, validation

I. INTRODUCTION

Electrathon America is an organization dedicated to promoting the design, development and construction of 100% electric vehicles for evaluation in competitions. These vehicles stand out for being light, efficient, and low-cost. Its main objective is to drive technological innovation and to provide students and electromobility enthusiasts with practical training in areas related to engineering, energy, and sustainability [1].

During the competition, vehicles are subjected to various tests that include technical inspections based on official regulations. This document emphasizes critical safety aspects that must be considered, especially in

chassis design. Subsequently, static tests are carried out to evaluate the structural performance of the vehicle.

The design and development of the chassis of a single-seater vehicle is a fundamental aspect in automotive engineering, as it directly influences the safety of the driver, the performance, and the efficiency of the vehicle. The chassis is the main structure responsible for supporting all the vehicle's systems and ensuring the integrity of the driver in the event of an impact [2].

To design an optimal chassis, it is essential to use simulation software to evaluate its safety, resistance, and reliability. These programs include Computer Aided Design (CAD) tools for modeling, Computer Aided Engineering (CAE) for Finite Element Method (FEM) analysis, and motion simulation software for advanced dynamic studies.

After a detailed analysis, the most critical tests to be carried out on a chassis have been identified:

- Side impact analysis;
- Frontal impact analysis;
- Scope Impact Analysis;
- Torsional stiffness analysis (either front or rear).

In addition, other structural assessments need to be considered, such as: roll bar analysis, front arch or roll bar analysis, flex analysis, acceleration analysis and braking analysis

Another key aspect in chassis design is material selection. It is not the same to use 6061-T6 aluminum as AISI 4130 steel; therefore, it is essential to make comparisons between materials to choose the best option in terms of weight, strength, and cost. Previous research highlights the importance of this analysis to ensure an efficient and safe design [3].

Regarding the design of vehicles for various competitions, there are several works on design and also on validation tests through simulation and experiments. In Electrathon vehicles, the goal is a safe, aerodynamic design, and, above all, a design with greater autonomy. The type and weight of batteries used are restricted; therefore, test and race speeds are low, around 40 km/h.

In the above context, various works on the design, simulation, and experimentation of vehicle chassis from different categories or competitions were reviewed. Das [4] designed a chassis for a student racing vehicle, considering rigidity, torsional rigidity, drive train layout, suspension points, driver position, and controls and safety. He obtained a redesigned model that addressed all of these aspects. Krzikalla *et al.* [5] carried out a test bench to measure torsional stiffness and subsequently compare simulation and experimental results, obtaining a very good approximation of the overall torsional stiffness with an uncertainty of less than 10%. Kumar *et al.* [6] designed a chassis and performed frontal, side, and rear impact tests considering two types of materials: 7075 aluminum alloy and 1023 carbon steel. They obtained better safety factor results in the various tests with the aluminum alloy. Chittaliya *et al.* [7] analyzed the racecar chassis design and performed safety factor, deformation, and stress analysis in front impact, rear impact, side impact, front torsional, rear torsional, static vertical bending, and lateral venting tests. A force of 5150.25 N was used for the front impact test and 3430 N for the other tests, all based on the vehicle weight. Sebastian *et al.* [8] simulated a chassis for SAE Formula using 4030 steel, 6061-T6 aluminum, and carbon fiber. They performed static and dynamic tests: frontal and side impact, torsion, braking, cornering, among others. The safety factor obtained was acceptable in all tests and a stiffness greater than 2500 Nm/deg. They obtained better stress distribution results in steel and greater strength in carbon fiber. Regarding studies on vehicle aerodynamics, Abinesh and Arunkumar [9] investigated the effect of aerodynamics on an intercity bus. They performed CFD analysis on the original model and a modified one, with the goal of reducing drag and fuel consumption. They reduced drag by 10% and reduced the fuel requirement by -16.33%. Recently, several studies have analyzed the structural integration of the battery pack in Battery Electric Vehicles (BEVs), which are a key element in improving the rigidity and safety of the chassis [10]. Scurtu and Moldovany [11] developed a conceptual design of the chassis of an electric vehicle by using the topology optimization method, with the aim of mainly reducing the structural mass while maintaining adequate mechanical performance. Their study analyzes different configurations of the chassis using steel and aluminum alloys as materials under representative load conditions, showing that topological optimization allows a more efficient distribution of the material, which helps in improvements in the rigidity and structural efficiency of the chassis. Singh [12] carried out a detailed review of the use of different metals and light alloys used in the manufacture of electric vehicles, where he highlights that materials such as aluminum, magnesium and titanium alloys offer a high strength-to-weight ratio, considerably improving energy efficiency and reducing the total mass of the vehicle. Several researchers have evaluated the use of aluminum alloys from the 6000 series as promising structural materials for the chassis of electric vehicles, due to their high strength-weight, good corrosion behavior, and ease of processing. In particular, different

6000-alloys under T4 and T6 heat treatments have been compared [13].

This work is divided into several stages, which are: the design of the car, manufacturing, assembly, electronics and performance tests (see Fig. 1). Based on the above, the design, structural analysis, manufacturing of the structure, and fluid flow analysis of the body are reported.

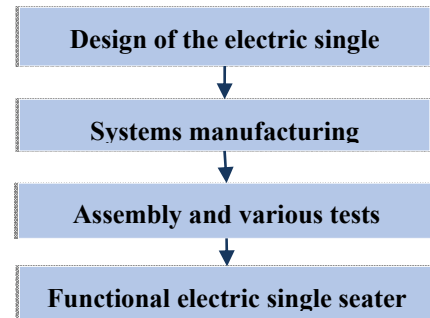


Fig. 1. Project development diagram.

II. MATERIALS AND METHODS

A. Guidelines Design

The following subsections describe each of the requirements of Electrathon America [1].

1) Dimensions and configuration of our design

In relation to the dimensions established in the Electrathon Americas regulations, our proposal considers a maximum length of 3.014 m, a maximum width of 1.219 m and a maximum height of 0.831 m, which are shown in Fig. 2.

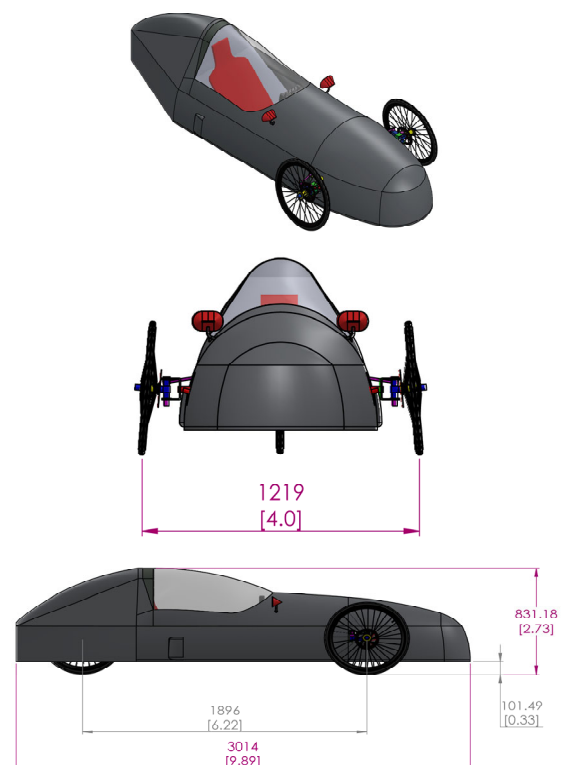


Fig. 2. General dimensions of the electric single seater.

The dimensions shown in the previous figure are within the Electrathon Americas regulations, which are indicated in Fig. 3.

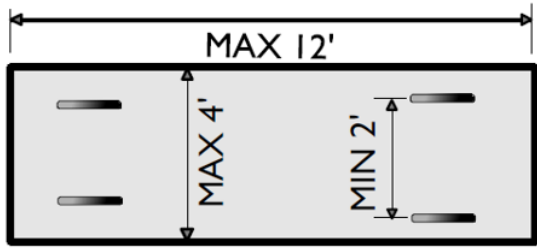


Fig. 3. Dimensions established by Electrathon Americas.

2) Single-seater frame and roll bar

To determine the critical interior dimensions of the electric single-seater cabin, a configurable virtual dummy model was chosen that emulates the characteristics of the pilot's position, size, and reach of the controls. This dummy is shown mounted on the vehicle in Fig. 4. To model this dummy, it was based on an individual weighing 81 kg, which is established in the Electrathon Americas regulations. The center of gravity is also shown in Fig. 4, which is longitudinally aligned with the center of the structure, located 654.9 mm from the rear axle and 152 mm above the chassis base.

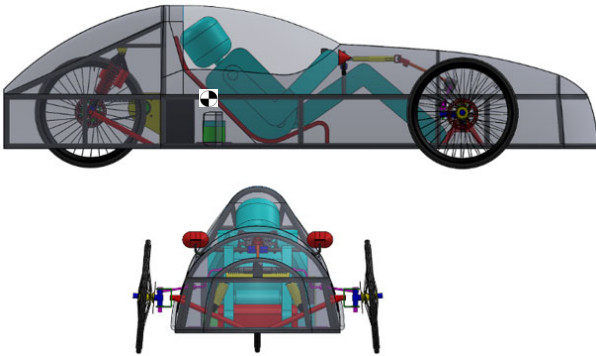


Fig. 4. Virtual dummy configured and mounted in vehicle.

In Fig. 5, it can be observed that the virtual model of the individual is used to compare section "4. ROLL BAR" of the "Electrathon America Regulations" document.

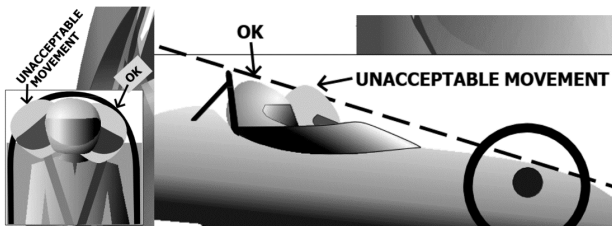


Fig. 5. Images of section "4 ROLL BAR" of the document "Electrathon America Regulations".

3) Chassis

The chassis can be defined as the skeleton of the car, since it is the internal structure that provides support,

rigidity, and the shape or design of the vehicle. It is also responsible for connecting the wheels and the steering system. This structure receives all the loads and stresses applied to the vehicle, in motion or rest. Its most important function is to safeguard the safety of the occupant traveling inside the vehicle.

The design of our chassis is shown in Fig. 6.

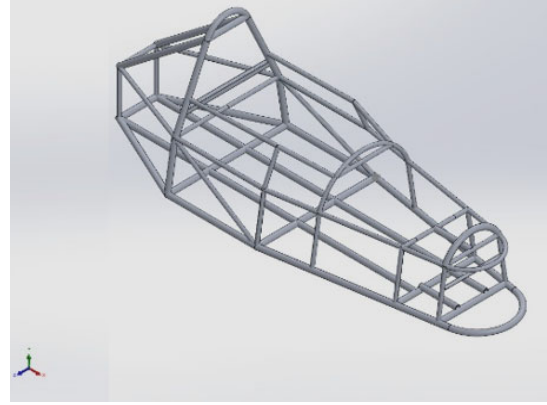


Fig. 6. Design of the single-seater structure.

B. Structural Analysis

The design of the chassis or frame depends on the application or type of vehicle to which it is to be applied.

The overall vibration of the car is related to the stiffness and mass distribution, therefore, to validate the design of our chassis, a pair of analyses was conducted out, one of torsion and one of bending. Furthermore, the selection of torsion and bending analyses was primarily based on the single-seater's operating conditions, namely an average speed of 35 km/h and the absence of collisions. Regarding the torsion analysis, the weight distribution of the car is considered between 40% and 60% for the front and rear, respectively [14, 15]. For our case, a total weight of the car was considered as 1471.5 N, which for the case of the analysis, results in a torque of $(1471.5 \text{ N}) \times (0.6\text{m}) = 882.9 \text{ Nm}$. The boundary conditions used in the simulation of the car structure are shown in Fig. 7.

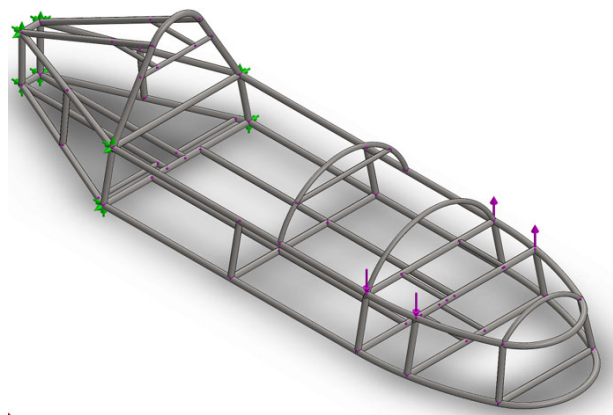


Fig. 7. Boundary conditions of the torsion analysis.

Table I shows the boundary conditions and their respective units.

TABLE I. UNITS AND BOUNDARY CONDITIONS

Load	Magnitude	Unit
Force	1000	N
Torsion	1471.5	Nm

It is important to mention that the following Eq. (1) was used to calculate the torsional stiffness.

$$K = (F \times L) / [\tan^{-1}[(\Delta y_1 + \Delta y_2) / 2L]] \quad (1)$$

Additionally, an analysis of the grid's independence and its corresponding error was performed, which is shown in Fig. 8.

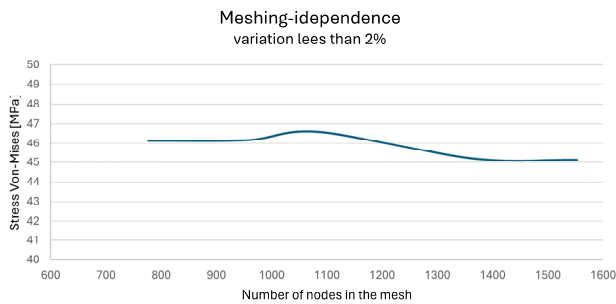


Fig. 8. Independence structural mesh.

C. Drag Analysis

The single-seater vehicle model was simplified by leaving only the outer surface of the body, as shown in Fig. 9, since it is on this surface where the greatest effects of the air flow around the vehicle develop.

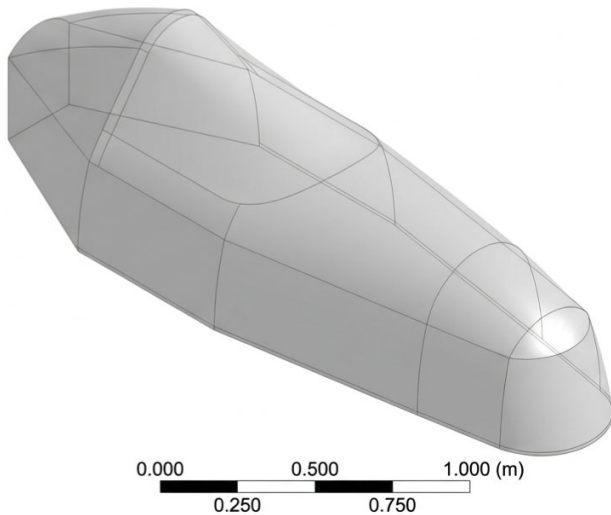


Fig. 9. Vehicle model to be analyzed in CFD.

A control volume was generated around the model simulating a wind tunnel measuring 12.5 m long, 5 m wide and 5 m high, as shown in Fig. 10. The size of this control volume allows enough space for the fluid flow to develop, resulting in faster and more accurate convergence.

Fluid analysis was performed in Ansys Workbench and tetrahedral elements for CFD-Fluent were used to mesh the control volume. The result of the domain

discretization allowed working with 444,369 elements and 81,027 nodes (Fig. 11).

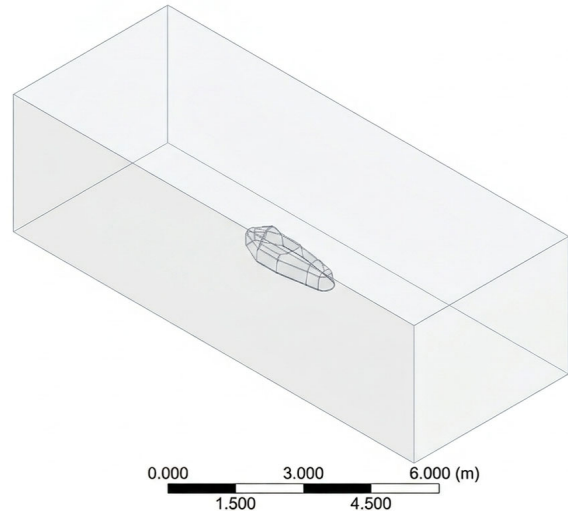


Fig. 10. Control volume around the vehicle model.

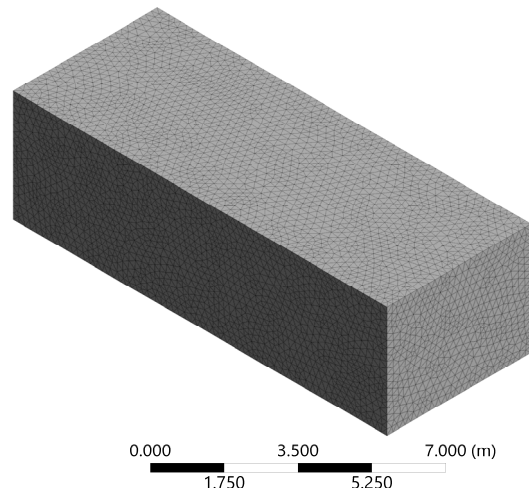


Fig. 11. Control volume mesh.

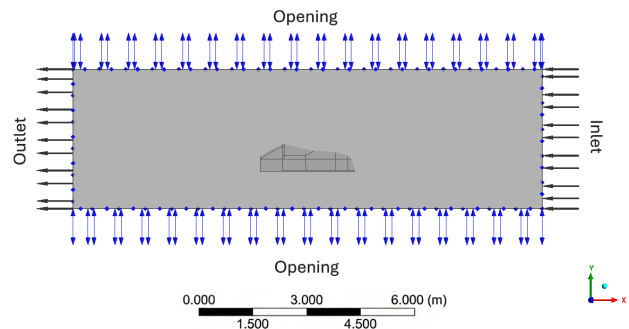


Fig. 12. Boundary conditions of the control volume.

The boundary conditions for the fluid simulation are shown in Fig. 12, where an air inlet velocity was applied, simulating that the vehicle moving at a speed from 10 to 60 km/h. The lateral, upper and lower sides of the control volume were indicated as openings, to avoid influences on the results that could occur if walls were used.

The turbulence model used in the fluid simulations is the Shear Stress Transport (SST) $k-\omega$, a widely used and

robust two-equation eddy viscosity turbulence model in computational fluid dynamics.

D. Chassis Manufacturing

Regarding the welding of the structure, first, the outline of the structure was drawn using 1:1 scale masking tape. Once the outline was completed, the cuts and folds were made to achieve the desired shape. Fig. 13 shows the methodology used, note that the longest tubes were placed longitudinally.



Fig. 13. Guide drawing of the structure to be manufactured.



Fig. 14. Fish-mouth cuts.



Fig. 15. TIG welding of the single-seater structure.

To perform the TIG welding, argon gas, filler material 4043 aluminum (1/8), and a green tip tungsten electrode were used. A characteristic of the welding in the structure was the joints: fish-mouth cuts were made to increase the mechanical resistance of the assembly. This was used in

all intersections, both transverse and towards the top, see Figs. 14 and 15.

E. Strain Gauges

To validate the results obtained through structural simulation, CEA-06-125UWA-120-type strain gauges were placed at the points where the greatest stresses occurred during the bending and torsion tests. The Vishay P3 was used in a quarter-bridge configuration with a Gauge Factor (GF) of 1.98 (Fig. 16). Strain G1 and G2 were placed 2.5 cm from the base of the single-seater, and G3 was placed 2 cm from the base.

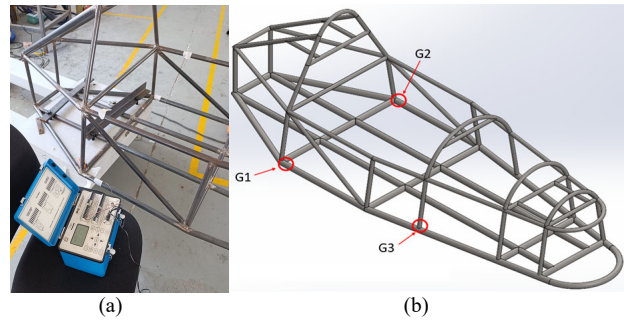


Fig. 16. Instrumentation. (a) arrangement for measuring microdeformations; (b) location of strain gauges.

F. Electrical Connections

The electrical diagram, shown in Fig. 17, represents the configuration of the single-seater's electrical system, highlighting both its connections and the functional integration of its multiple components. The power source comes from a 1 kW battery, connected to the motor through a 2 kW controller, which efficiently manages the energy transfer. The electrical system incorporates a Smart Battery Management System (BMS) with Bluetooth connectivity, allowing remote monitoring of the battery status through a dedicated mobile app. This tool provides real-time information on critical parameters such as charge level, total and per-cell voltage, internal battery temperature, charge and discharge current, number of charge cycles, alarms for overload, over-discharge, over-temperature, and other faults.

G. Tests and Improvements

After conducting various tests on a track, and following two national races, the Electratón América 2024 and 2025, proposals for improvements were made, primarily in weight reduction and aerodynamics. The proposed improvements are shown in Fig. 18. The modifications were made to the rear of the vehicle: the suspension system was replaced with aluminum components, the steel rims were replaced with aluminum, the body was replaced from fiberglass to aluminum sheet metal, and most steel components were made of aluminum to reduce weight. Furthermore, the front of the electric single-seater was modified to improve aerodynamics.

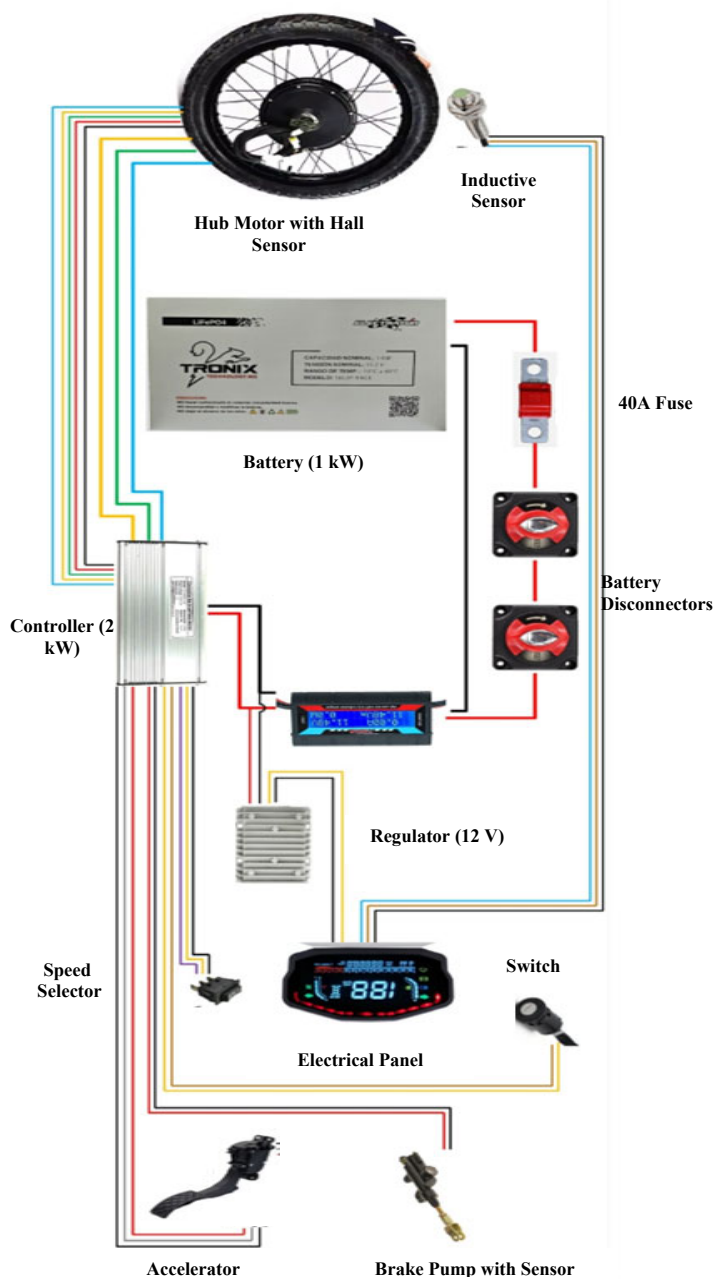


Fig. 17. Vehicle electrical diagram.

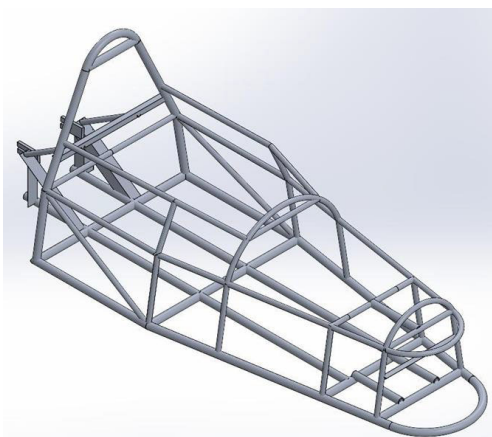


Fig. 18. Optimization of the single-seater structure.

TABLE II. PARAMETERS OF TEST CONDITIONS

Conditions	Value
Test track length	400 m
Race track length	900 m a 1200 m
Driver weight	81 Kg
Race duration	1 hour
Environmental conditions	25 °C
Battery	Voltage and amperage check
Software BMS Smart	Calibration check

Regarding the test data, Table II present the test data and components of the single-seater.

III. RESULT AND DISCUSSION

Fig. 19 shows the result of the deformation produced by the torque of 1471.5 N. The maximum displacement at the ends of the single-seater chassis is 11.7 mm with a twist angle of 1.92 degrees.

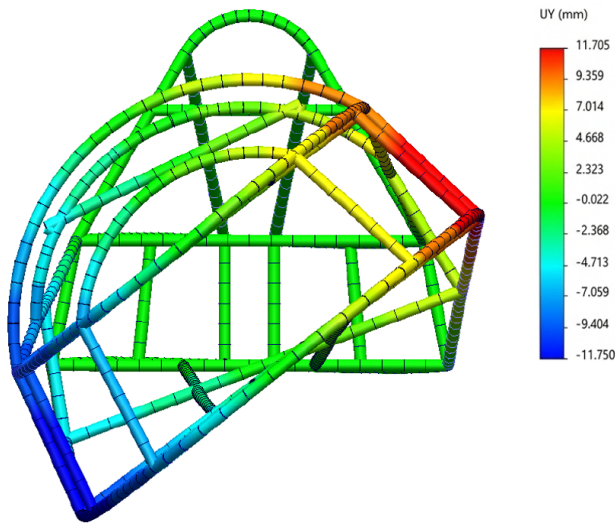


Fig. 19. Deformation of the single-seater structure.

Based on these results and using Eq. (1) to calculate the torsional stiffness, it was determined that the rigidity of the single-seater chassis is 657 Nm/deg, which is similar to results obtained by other authors, for example Krzikalla *et al.* [5, 15], obtains in the simulation a torsional stiffness of 646 Nm/deg and in the experimental one of 679 Nm/deg.

Fig. 20 shows a maximum displacement due to bending load of 0.2 mm.

Within the stress analysis of the structure, the maximum stress was found to be 46.5 MPa, with a minimum safety factor of 7.5, as shown in Fig. 21.

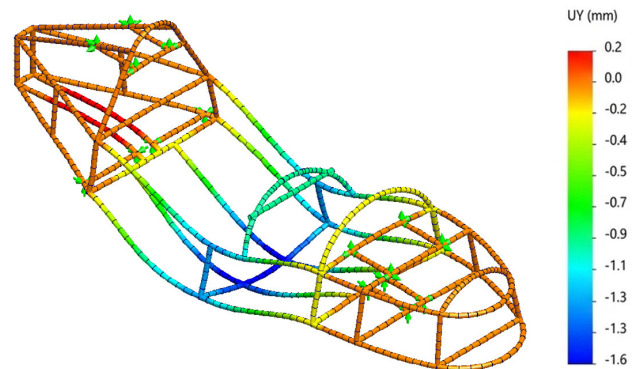


Fig. 20. Bending displacement of the single-seater structure.

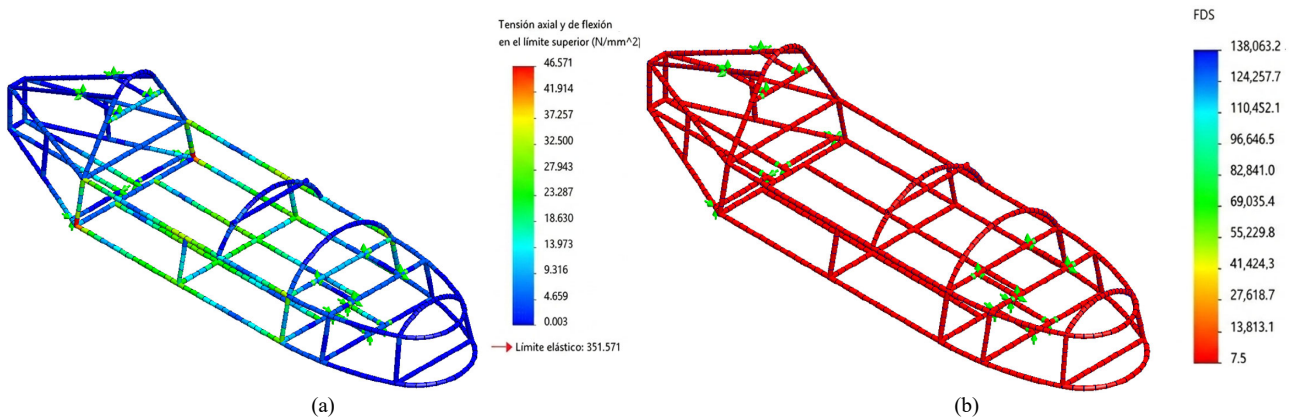


Fig. 21. Bending analysis. (a) stress state; (b) safety factor.

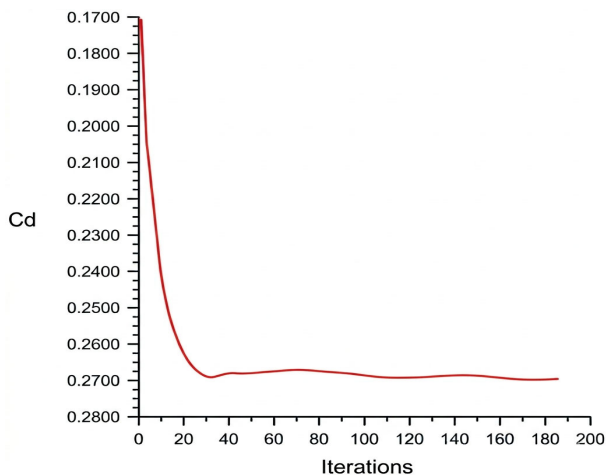


Fig. 22. Convergence of the drag coefficient of the vehicle at a speed of 60 km/h.

Convergence in most simulations did not exceed 185 iterations thanks to the simplification of the model and the appropriate size of the control volume. One of the most significant results of the fluid analysis is presented in Fig. 22, where the convergence plot of the drag coefficient is shown for the vehicle moving at a speed of 60 km/h.

The simulation results show that drag coefficient increases as the vehicle's travel speed increases, as shown in Fig. 23. Using a trend line with a power-law function, an equation can be obtained that allows the drag coefficient of the vehicle's to be determined at any speed.

The drag coefficient is related to the surfaces of the body that exert the greatest resistance to the air flow around the vehicle, and the highest pressures are also present on these surfaces. Fig. 24(a) shows that the maximum pressure of 168.8 Pa occurs at the front of the

vehicle, precisely where the slowest flow is shown in Fig. 24(b). The opposite is true for the widest part of the vehicle, where the lowest pressure is present due to the high speeds of the air flow.

Fig. 23(b) also shows that turbulence is relatively low due to the aerodynamic shape of the vehicle, which is generated at the rear due to the detachment of the boundary layer of the air flow.

To obtain the power required for the vehicle to overcome air resistance, it was necessary to determine its frontal area, which is 0.469 m² (Fig. 25).

The power required for the vehicle to overcome air resistance is shown in Fig. 26, where it can be seen that the vehicle requires a power of 1300 W to move at 60 km/h.

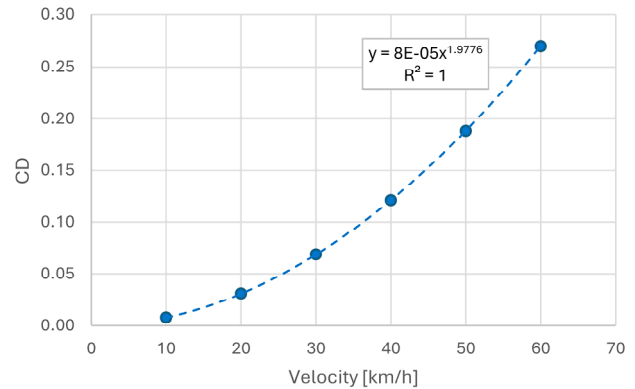


Fig. 23. Behavior of the drag coefficient during vehicle operating speeds.

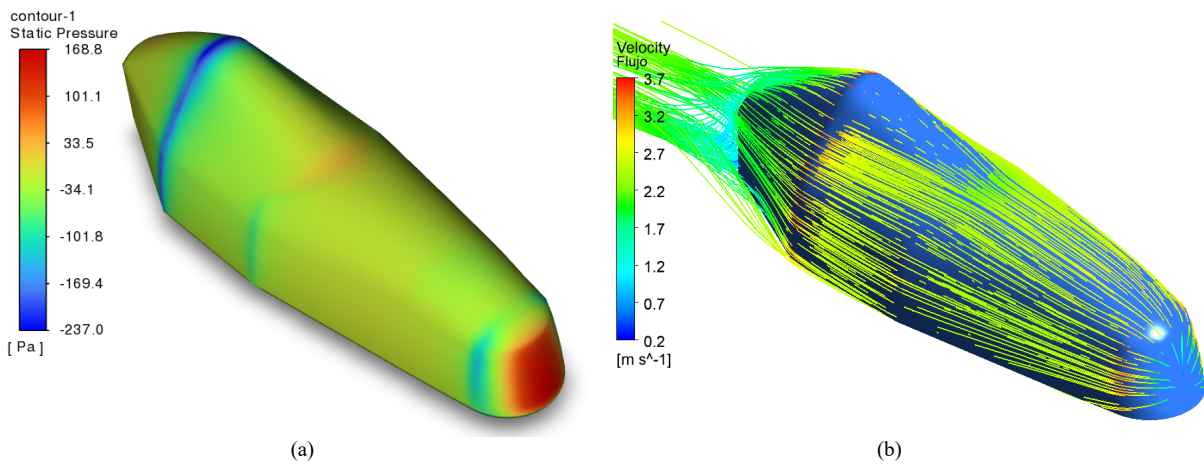


Fig. 24. Aerodynamic behaviour on the surface of the vehicle at a speed of 60 km/h. (a) pressure distribution; (b) flow speed.

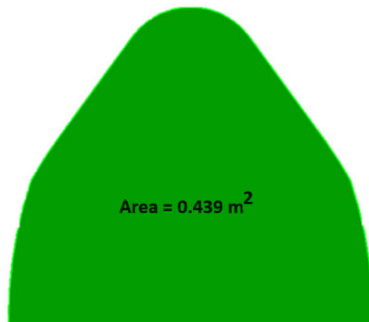


Fig. 25. Frontal area of the vehicle.

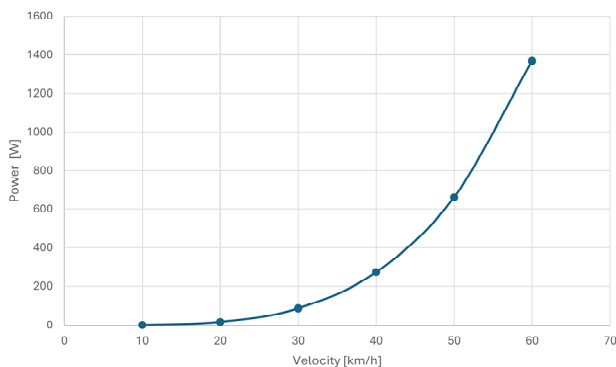


Fig. 26. Power required to overcome air resistance.

The experimental results and simulation are similar, except for Gauge 3 (G3). In Fig. 27, it can be observed that the simulated for G3 is 9.048 MPa, while the experimental value is 9.6 MPa, resulting in a qualitative error of 5.75% which indicates a very high agreement between the values.

The finished chassis is shown in Fig. 28, with a total weight of 16 kg.

Finally, after completing all the research, manufacturing, and assembly activities, a functional vehicle was obtained (Fig. 29).

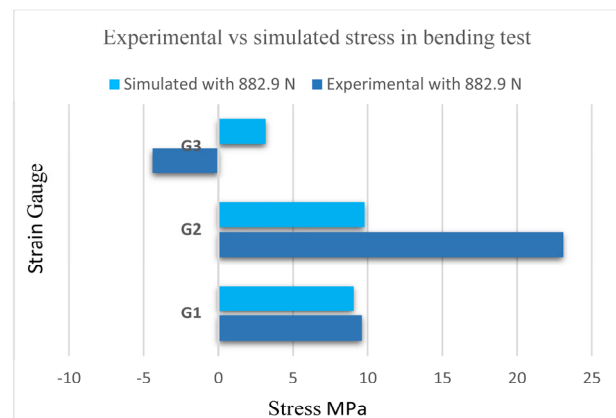


Fig. 27. Comparison of values experimental and simulated.



Fig. 28. Aluminum structure of the single seater completed.



Fig. 29. Developed single-seater.



Fig. 30. Improved single-seater.

With improvements in weight and aerodynamics, the maximum speed reached in competition was 45 km/h and the average speed was 35 km/h, as demonstrated by the single-seater shown in Fig. 30.

IV. CONCLUSION

A functional electric vehicle was obtained and used for Electrathon America competitions through the appropriate integration of CAD-CAM-CAE technologies

for structural design, electrical system integration, assembly processes, and aerodynamic optimization. The development of the electric vehicle meets the established requirements, ensuring proper on-track performance.

During the vehicle's development, it was determined that the two main factors affecting the single-seater's range are weight and aerodynamics. On the one hand, weight reduction was addressed by manufacturing the chassis using 6061-T6 aluminum tubular profiles. On the other hand, aerodynamics were analyzed through CFD simulations, resulting in an optimized body design for the electric single-seater. Consequently, several improvements were achieved, including an increase in maximum speed from 33 km/h to 45 km/h, a reduction in vehicle weight from 135 kg to 86 kg (a 36% reduction), and a decrease in the drag coefficient. Reducing the thickness of the tubular profiles was considered; however, this approach would have led to a loss of structural strength and, consequently, a reduction in the safety factor. The use of carbon fiber was also evaluated but was deemed economically unfeasible. Overall, these improvements increased the vehicle's range by 39.8%, resulting in enhanced competitive performance.

The stress predictions for the electric vehicle's structure are consistent with the numerical results, thereby validating the analyses performed. It is important to note that the safety factor for the aluminum structure is 1.7, which ensures optimal performance and provides confidence in the vehicle's structural reliability.

Additionally, the single-seater successfully passed design, safety, manufacturing, and performance evaluations conducted by Electrathon and the FIA (International Automobile Federation). The optimized vehicle achieved first place in the national Electrathon 2025 Beyond Frontiers Championship in the America category.

Finally, the project highlights the development of human resources in this field, enabling future participation in electric vehicle development within the country. The active involvement of 15 students, primarily from the Robotics Engineering program, is particularly noteworthy.

CONFLICT OF INTEREST

The authors declare no conflict of interest.

AUTHOR CONTRIBUTIONS

VGA led the project and participated in the instrumentation, manufacturing, design and manuscript preparation; FJSB performed the design, stress analysis and fluid analysis; PJSJ performed stress and dynamic analysis; PYC supported the manufacturing of the structure; AAGP conducted investigations, stress analysis, and instrumentation task; all authors had approved the final version.

ACKNOWLEDGMENT

The authors would like to thank the University Polytechnic of Guanajuato and the members of the E

UPG MOTORS team. Recognize IECA-INGENIUM for their support with the fabrication of electric vehicle structure.

REFERENCES

- [1] *Electrathon America*, ELECTRATHON AMERICA RULEBOOK, Rev. K, Michael-Lewis, USA, 2021, pp. 3–38.
- [2] H. Hazimi, Ubaidillah, A. E P. Setiyawan *et al.*, “Vertical bending strength and torsional rigidity analysis of formula student car chassis,” in *Proc. 3rd Int. Conf. on Industrial, Mechanical, Electrical, and Chemical Engineering*, 2018, vol. 1931, 030050.
- [3] A. S. F. Martínez, A. M. S. Castrillón, and S. A. S. Castrillón, “Analysis of the chassis structure of a formula student racing car,” *Int. J. Eng. Res. Technol.*, vol. 14, no. 10, pp. 1005–1017, 2021.
- [4] A. Das, “Design of student formula race car chassis,” *Int. J. Sci. Res.*, vol. 4, no. 4, 2015.
- [5] D. Krzikalla, J. Mesicek, J. Petru *et al.*, “Analysis of torsional stiffness of the frame of a formula student vehicle,” *Appl. Mech. Eng.*, vol. 8, no. 1, 315, 2019.
- [6] G. J. Kumar, V. Aditya, K. P. Kumar *et al.*, “A study on the analysis and optimization of vehicle chassis,” *Int. J. Adv. Res. Innov.*, vol. 9, no. 2, pp. 68–75, 2021.
- [7] S. Chittaliya, H. Anghan, and U. Vaghani, “A methodological study to analyze and design the car chassis,” *Int. J. Res. Appl. Sci. Eng Technol.*, vol. 9, pp. 390–394, 2021.
- [8] A. Sebastian, A. Miyaer and A. Suarez, “Analysis of the chassis structure of a formula student racing car,” *Int. J. Eng. Res. Technol.*, vol. 14, pp. 1005–1017, 2021.
- [9] J. Abinesh and J. Arunkumar, “CFD analysis of aerodynamic drag reduction and improve fuel economy,” *International Journal of Mechanical Engineering and Robotics Research*, vol. 3, no. 4, pp. 430–440, 2014.
- [10] G. Belingardi and A. Scattina, “Battery pack and underbody: integration in the structure design for battery electric vehicles—Challenges and solutions,” *Vehicles*, vol. 5, no. 2, pp. 498–514, 2023.
- [11] I. L. Scurtu and D. Moldovanu, “Conceptual design of an electric vehicle chassis using topology optimization method,” *IOP Conf. Series: Materials Science and Engineering*, 2024, vol. 1311, no. 1, no. 012022.
- [12] R. Singh, “Lightweight metals and alloys in electric vehicle manufacturing: Enhancing performance and efficiency,” *Int. J. Sci. Res. Archiv.*, vol. 13, no. 02, pp. 1735–1742, 2024.
- [13] F. E. Saldanha, S. de A. Sousa, G. L. de Gouveia *et al.*, “Evaluation of 6000 aluminum alloys for application in chassis of electric vehicles,” *Materials Research*, vol. 25, e20220275, 2022.
- [14] A. Ghosh, R. Saha, S. Dalhi *et al.*, “Structural analysis of student formula race car chassis,” *International Research Journal of Engineering and Technology* vol. 5, pp. 1268–1273, 2018.
- [15] D. Krzikalla, A. Slíva, J. Měšicěk *et al.*, “On modelling of simulation model for racing car frame torsional stiffness analysis,” *Alexandria Eng. J.*, vol. 59, pp. 5123–51333, 2020.

Copyright © 2026 by the authors. This is an open access article distributed under the Creative Commons Attribution License which permits unrestricted use, distribution, and reproduction in any medium, provided the original work is properly cited ([CC BY 4.0](https://creativecommons.org/licenses/by/4.0/)).